# Mg ordering, reaction, and crystallite formation on GaAs(110): Scanning tunneling microscopy and photoemission studies

Y. Z. Li, J. C. Patrin, Y. Chen, and J. H. Weaver
*Department of Materials Science and Chemical Engineering, University of Minnesota, Minneapolis, Minnesota 55455*
(Received 15 April 1991)

The coverage-dependent growth structures formed by Mg deposition on GaAs(110) have been studied using scanning tunneling microscopy (STM) and synchrotron-radiation photoemission. In the low-coverage regime at 300 K, Mg adatoms bond on a bridge site between one Ga and two As surface atoms to form two-dimensional domains with local $2\times1$ structure. Dual-bias STM imaging shows a higher density of unoccupied states than occupied states for these Mg atoms, indicating charge transfer from Mg to the substrate. This $2\times1$ overlayer is replaced by three-dimensional clusters when the local atom density increases and chemical intermixing is initiated. With increased Mg deposition, the heterogeneous surface region becomes more uniformly reacted and the clusters coalesce. By $\sim$10-monolayer deposition, the resulting polycrystalline film is locally smooth, although atomic height steps are evident and there are a large number of dislocations.

## INTRODUCTION

Scanning tunneling microscopy (STM) has been used to investigate the formation of metal-semiconductor interfaces, allowing direct observation of long- and short-range overlayer order in real space.[1–9] In principle, overlayer growth structures are determined by adatom-adatom and adatom-substrate interactions, with constraints related to kinetics. The adatom-adatom interactions can be estimated by the bulk cohesive energy but adatom-substrate interactions reflect the number of adatoms present locally and cannot be characterized by a macroscopic parameter.

This study focuses on one of the parameters that influences the growth mode: the cohesive energy of the overlayer. We have studied the interaction of Mg with GaAs(110) because Mg has a very low cohesive energy. We speculated that the Mg growth mode could be predicted by reviewing the growth modes of Cs (group I) and Al (group III) on GaAs(110). It has been shown that Cs atoms deposited at 300 K form zigzag chains along the substrate $[1\bar{1}0]$ direction.[6] Such two-dimensional (2D) growth is related to the optimal configuration of stable nuclei. In contrast, Al atoms form three-dimensional (3D) clusters[10] because Al-Al bonding is favored over Al-GaAs bonding. From the intermediate cohesive energy of Mg, we expected 2D growth for Mg on GaAs(110). [The cohesive energy of Cs is very low (0.8 eV/atom), that of Mg is higher (1.51 eV/atom), and that of Al is comparatively high (3.39 eV/atom).] At the same time, the prospect of interfacial reaction could be inferred from results for Ca/GaAs(110).[11] Hence, we were interested in the interplay between overlayer ordering and reactive intermixing for increasing amounts of Mg on the surface.

Three distinct growth regimes were observed for Mg/GaAs(110). Two-dimensional growth dominated at very low coverage where an ordered $2\times1$ structure was observed and at very high coverage where oriented Mg crystallites were observed with well-defined steps and dislocations. Equally interesting was the intermediate regime between $\sim$0.25 and $\sim$10 ML (where ML denotes monolayer) because clusters were observed with STM and intermixing of Mg, Ga, and As due to interfacial chemical reactions was demonstrated with photoemission.

## EXPERIMENT

The STM experiments were conducted using a commercial instrument[12] in an ultrahigh-vacuum system of base pressure $\sim6\times10^{-11}$ Torr. GaAs(110) surfaces were prepared by *in situ* cleaving of *p*-type single-crystal posts doped with Zn at $2\times10^{18}$ cm$^{-3}$. Mg was sublimed from a resistively heated tantalum boat. The typical deposition rate was $\sim$1 Å/min at low coverage and $\sim$4 Å/min at high coverage. Overlayer growth was done at room temperature, and the pressure in the chamber remained below $5\times10^{-10}$ Torr. Metal coverages were measured with a quartz crystal thickness monitor. The coverage of 1 ML was defined to be one adatom per substrate Ga or As atom. This yields a surface monolayer density of $8.86\times10^{14}$ atoms cm$^{-2}$, leading to a conversion factor of 2.0 Å/ML for Mg. STM tips were prepared by electrochemical etching of tungsten wires of 0.5 mm diameter. The tips were annealed by electron bombardment before every experiment. Tip bias voltages were $\pm$(2.4–3.0) V and the tunneling current was typically 0.1–1.0 nA. Single lines were scanned with a typical frequency of 2–4 Hz. The atomic structure of the substrate was determined by dual-bias imaging of Ga and As surface atoms.[13]

The synchrotron-radiation photoemission experiments were conducted in a spectrometer at the Wisconsin Synchrotron Radiation Center. Photoelectrons were collected with an angle integrated double-pass cylindrical mirror analyzer, as described elsewhere.[14] The overall energy resolution, controlled by selecting monochromator slits and analyzer bandwidth, was 0.25 eV for Ga 3*d*, As

 

3*d*, and Mg 2*p* core-level energy distribution curves (EDC's). These EDC's were analyzed with an IBM RT computer using a nonlinear-least-squares-minimization curve-fitting routine.[15]

## STM STUDY OF GROWTH STRUCTURES

### Mg adsorption structures

Figures 1(a) and 1(b) show images of the occupied and unoccupied states for 0.12 ML Mg deposited at 300 K onto GaAs(110). These 140×140 Å$^2$ STM images were acquired with tip bias voltages of 2.4 and −2.4 V and tunneling currents of 0.7 nA from the same surface area. The regular lattice in the background is the atomically resolved GaAs(110) surface, imaging As atoms as in Fig. 1(a) and Ga atoms in Fig. 1(b). The bright features that appear as small two-dimensional arrays represent Mg adatom. Comparison of Figs. 1(a) and 1(b) shows a significant difference in the brightness of the Mg features, indicating an apparent adatom height difference between occupied and unoccupied state images. In particular, a Mg adatom measured <0.5 Å high in Fig. 1(a) but ~2 Å in Fig. 1(b). This difference in apparent heights between occupied and unoccupied state images was observed throughout the bias voltage range (~2–3.5 V) within which imaging could be achieved in these experiments. Such bias-dependent sizes have been discussed by Lang[16] and Hamers.[17] Since the height of a feature in an STM topograph relates to the surface density of states,[18] the difference indicates that the density of unoccupied states for Mg adatoms is greater than for occupied states at these biases. This suggests charge transfer from Mg to the substrate. Such charge transfer is also evident in the core-level photoemission data, which will be discussed later in this paper.

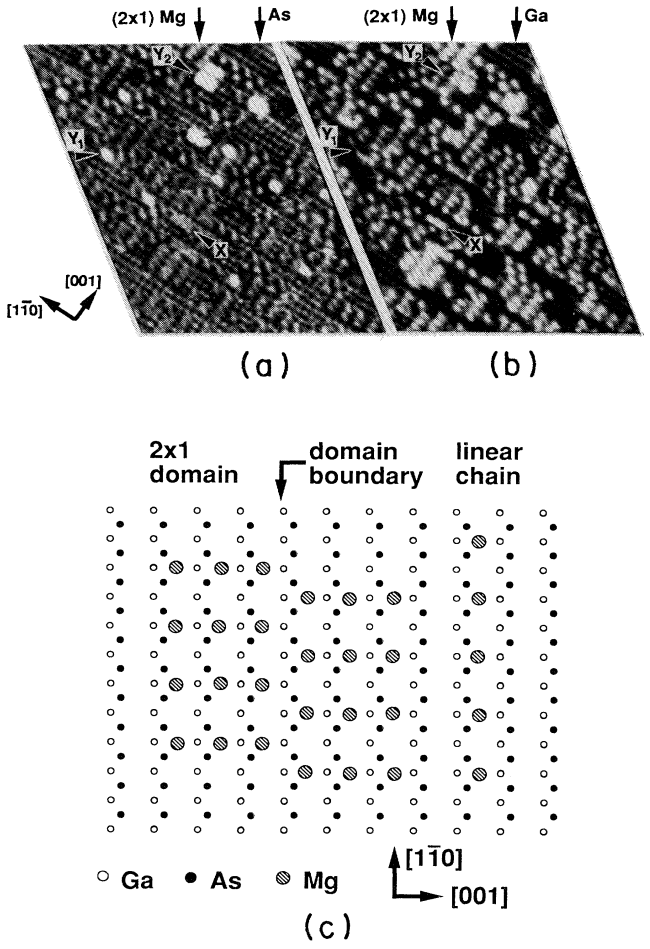


FIG. 1. STM images probing (a) occupied states and (b) unoccupied states of the same 140×140 Å$^2$ for 0.12-ML deposition of Mg on GaAs(110). The images were acquired with the tip biased by ±2.4 V and a constant tunneling current at 0.7 nA. Most Mg adatoms appear as individual bright features occupying the surface sites indicated in the schematic model of (c). The nearest-neighbor distances between Mg atoms are 8 and 5.65 Å along [1$\bar{1}$0] and [001] directions, respectively. The dominant structures reflect a local 2×1 array but linear chains along the substrate [1$\bar{1}$0] direction are also evident. The different brightnesses for Mg atoms in (a) and (b) reflect a higher density for unoccupied states than occupied states. Features marked *X* signal closer packing of Mg atoms in the [1$\bar{1}$0] direction while those marked *Y* signal nucleation of clusters.

Analysis of the STM images shows that individual Mg atoms adsorb on a bridge site between one Ga and two As surface atoms, as depicted in Fig. 1(c), with the surface [1$\bar{1}$0] and [001] directions as indicated. We arrived at this adsorption structure based on the assumption that the protruding features in the STM images truly represent the location of the Mg atom cores. The Mg atoms form two-dimensional arrays with a 2×1 structure with respect to the GaAs(110) substrate, starting at much lower coverages than shown in Fig. 1. Such ordering reflects the high atomic surface mobility of Mg. Linear chains comprised of as many as five Mg atoms were also observed to form along [1$\bar{1}$0] at lower coverage, as shown at the right of Fig. 1(c). This can be caused by a higher accommodation at the end of the linear chain or a lower diffusion barrier along the [1$\bar{1}$0] direction, as predicted for Al diffusion on GaAs(110).[19] The domains of the 2×1 structure were as large as 20×20 Å$^2$. When adjacent domains meet there is a 50% chance that an antiphase domain boundary will form. In this case, the atomic arrangement has a zigzag structure, as sketched in Fig. 1(c). The zigzag structure resembles the growth pattern for Cs, Sm, and Yb on GaAs(110),[6,8,20] but no isolated zigzag chains or large domains of the zigzag structure were observed because the structure is a consequence of the abutting of 2×1 domains.

The distance between Mg adatoms in the 2×1 structure is 5.65 Å along [001] and 8.0 Å along [1$\bar{1}$0], as shown in Fig. 1(c). The nearest-neighbor distance, 5.65 Å, is too large for direct Mg-Mg bonding, and interaction between Mg adatoms must be mediated by the substrate. This is analogous to what has been proposed for Cs on the (110) surfaces of GaAs and InSb.[6,21]

### Cluster nucleation and growth

The STM images show that most Mg adatoms deposited at 300 K form domains with a 2×1 structure at 0.12

ML coverage but also that a small number of other features are formed. One corresponds to a chain along $[1\bar{1}0]$ with an interatomic spacing of 4.0 Å, as indicated by $X$'s in Figs. 1(a) and 1(b). These appear differently from the $2\times1$ structures because the nearest-neighbor distance is reduced by a factor of 2. The apparent height for the $X$ features was the same as for $2\times1$ structures, based on occupied and unoccupied state images. Another feature, labeled $Y$ in Fig. 1, appears as a protrusion in occupied state images. Some of the $Y$ features are bright protrusions that resemble individual adatoms ($Y_1$) while others are agglomerates of individual bright features ($Y_2$). Both measure ~2 Å high in occupied state images [Fig. 1(a)] but they do not show discernible elevation in the unoccupied state images [Fig.1(b)]. These density-of-states characteristics distinguish $Y$ features from $X$.

Comparison of the $2\times1$ growth structure to the $X$ and $Y$ features shows that the major change is the nearest-neighbor distance. We postulate that weak Mg-Mg interactions responsible for the $2\times1$ structures are modified when additional Mg atoms are inserted to form denser arrays, such as $X$. The $Y$ aggregrates probably represent Mg atom addition on $X$ features as second layer growth. The $Y$ features seem most likely to promote nucleation and the growth of larger 3D clusters because of the high local Mg atomic density of $Y$ features.

The $X$ and $Y$ features of Fig. 1 occur rarely with 0.12-ML Mg deposition, but the density of $Y$ features increases rapidly with coverage and larger clusters form. Figure 2 shows a $170\times170$ Å$^2$ area after the deposition of 0.25 ML with an occupied state image on the left and an unoccupied state image on the right. Clearly evident are bright features ~20 Å in diameter and 2–4 Å high that indicate cluster growth. No evident order can be seen within the clusters. At this coverage, the clusters appear as protrusions in both occupied and unoccupied states' images, and this is different from the appearance of the $Y$ features that serve as nuclei of clusters. $Y$ features indicated by arrows in Fig. 2(a) are recognizable because they are bright in the occupied state images but not in the unoccupied state images. Areas away from the clusters and the $Y$ features exhibit unperturbed $2\times1$ structures identical to those of Fig. 1. Although STM cannot determine what elements make up the clusters, photoemission results allow an assessment of chemical interactions between Mg and GaAs(110), as will be discussed below.

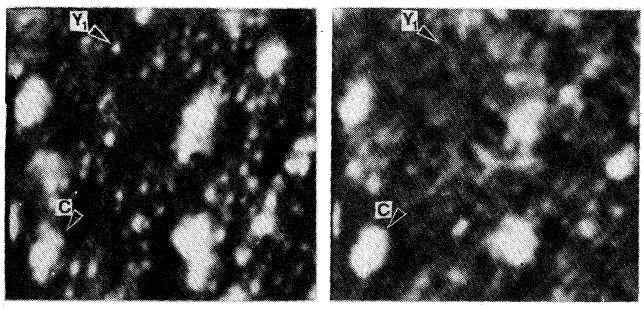


FIG. 2. STM images showing cluster formation after the deposition of the equivalent of 0.25 ML of Mg. The same $170\times170$ Å$^2$ was scanned with the tip bias of $\pm2.88$ V for (a) and (b), respectively, and a tunneling current of 0.15 nA. Clusters measuring ~20 Å in diameter and 2–4 Å in height with no apparent internal structure (marked $C$) can be seen along with unperturbed $2\times1$ areas and $Y$ features as in Fig. 1 (e.g., $Y_1$ marked). The photoemission results indicate that the clusters reflect intermixed regions containing Mg, Ga, and As.

The eight panels of Fig. 3 show the Mg morphology when the amount of Mg is increased from 0.25 to 30 ML. The images measure $290\times290$ Å$^2$ for 3(a) and $700\times700$ Å$^2$ for 3(b)–3(h). Figure 3(a) represents the unoccupied state with 0.25 ML Mg, showing that the surface is covered with $2\times1$ structures and the number of clusters is small. (The $2\times1$ structures appear as lines running from the lower left to the upper right in the image; the spacing between adjacent lines is 8 Å.) The coexistence of $2\times1$ regions and clusters indicates significant Mg adatom mobility on the $2\times1$ structure until cluster growth occurs, most likely at $Y$ features. Increased deposition yields more and larger clusters that cover the $2\times1$ structure. The images of Figs. 3(b), 3(c), and 3(d) were typical for the occupied states for $\theta=0.38$, 1, and 3 ML, respectively, where the clusters were 5–7 Å in height. The cluster heights did not increase at higher coverage but there was lateral growth and cluster coalescence to seal the surface, as in Figs. 2(e) and 2(f) for $\theta=5$ and 7.5 ML. The surface maintains the same roughness on a large scale at 9 ML but local smoothing is evident, as shown in Fig. 3(g). Atomic height steps also form, and this is an indication of the growth of ordered crystals. The crystalline character was apparent at 30 ML, as shown in Fig. 3(h), because large flat regions were observed and they were separated by atomic steps. A striking characteristic of these surfaces was the large number of dislocations, including the screw dislocations marked by arrows (next section).

Low-energy electron diffraction (LEED) investigations were also done in parallel with the STM studies. A clear $1\times1$ LEED pattern was observed for cleaved GaAs(110) but Mg deposition rendered the LEED spots fuzzy. No superstructure was observed and the substrate spots disappeared into a diffuse background by ~2-ML deposition. The absence of a detectable $2\times1$ LEED pattern at low coverage reflects the fact that the ordered domains were only $20\times20$ Å$^2$ in size. This is evident in Fig. 3(a) where small, imperfect $2\times1$ domains appear. Mg deposition above 30 ML produced a circular LEED pattern on a diffuse background indicative of polycrystalline Mg.

### Polycrystalline Mg film formation

Figure 3(h) shows that Mg coverages of ~30 ML produce a surface with numerous steps that originate primarily from dislocations, especially screw dislocations. Images of the terraces do not show atomic resolution, presumably because the electronic states of Mg are delocalized. For the steps, the measured height was 2.6 Å, in agreement with the height of a single step along the $c$ axis of hcp Mg. Results for Mg films of thickness 60 and 200

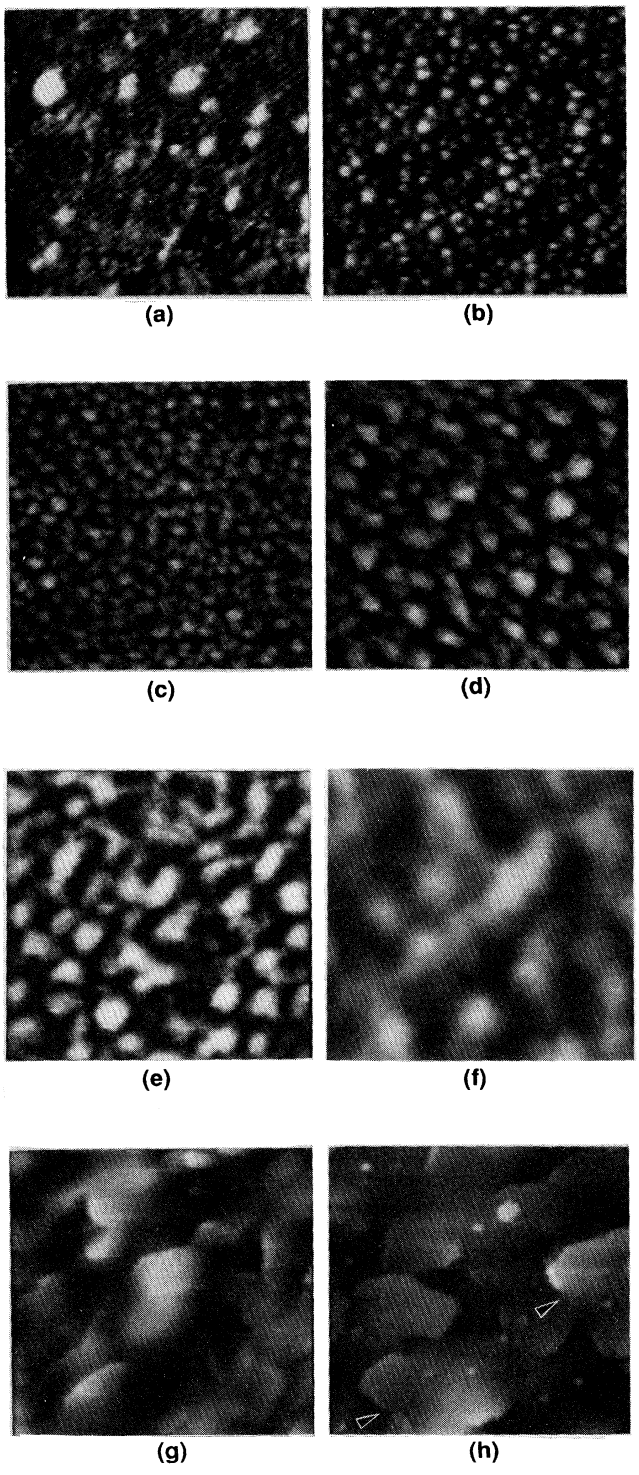


FIG. 3. STM images showing the evolution of the Mg/GaAs interface for deposition of 0.25, 0.38, 1.0, 3.0, 5.0, 7.5, 9, and 30 ML for images (a)–(h). The imaged region measured 290×290 Å$^2$ for (a) and 700×700 Å$^2$ for (b)–(h). Image (a) was acquired with a negative tip bias, but the others were taken with a positive tip bias. 2×1 structures observed at low coverages yielded to reacted clusters that grew laterally and eventually sealed the surface so that polycrystalline Mg film growth could occur. Arrows (h) indicate screw dislocations in the Mg film.

ML showed that the terraces and steps were defined by straight line segments. Straight step edges intersected at angles of 120°, consistent with growth of a hexagonal close-packed structure. Apparently, surface free energies favor the formation of straight edges on a close-packed crystal orientation. When all straight step edges are considered, however, their directions are random, as expected for polycrystalline growth.

The polycrystalline growth of Mg on GaAs(110) stands in contrast to what has been observed for other metals, including Sn,[5] Ag,[9] and Al.[10] For Mg, the flatness of terraces and the straightness of steps indicate high Mg surface mobility. This is not surprising since the activation energy is proportional to the bulk cohesive energy. This also accounts for surface smoothing as the clusters grew laterally. The transition from cluster to crystalline growth probably introduces dislocations because the clusters were disordered. Mobile Mg adatoms bond to dislocations and steps, thus sustaining layer-by-layer growth. Screw dislocations, which were observed for Mg films as thick as 200 ML, most likely propagate from the buried interface.

The STM images showed that the surface regions were stable, but we did observe changes more than 30 min after the films had been grown. Figure 4 shows two pairs of images that demonstrate such dynamic changes. Figures 4(a) and 4(b) are 1400×1400 Å$^2$ images for 15 ML

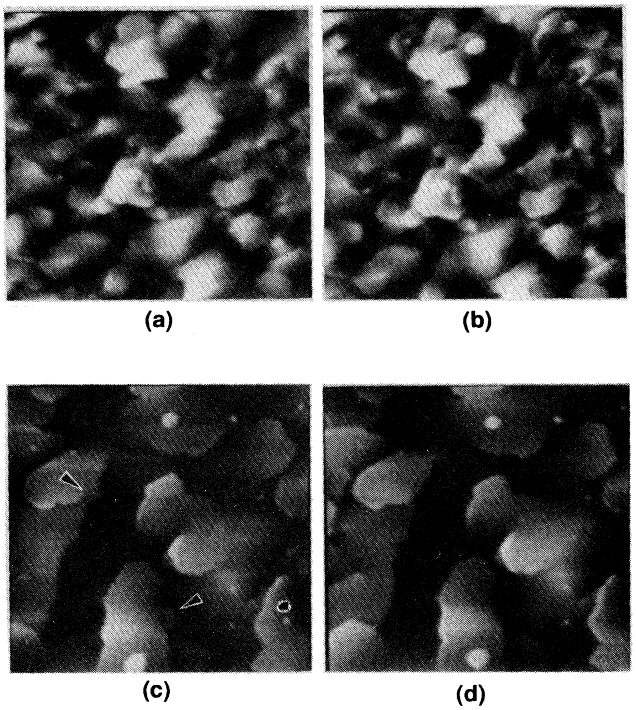


FIG. 4. These images highlight areas of structural instability and dislocation movement in the Mg thin films. Images (a) and (b) were taken ~2 min apart for the same 1400×1400 Å$^2$ area after 15-ML Mg deposition. Apparent structural changes occurred in the upper right portion. Images (c) and (d) were acquired from an 860×860 Å$^2$ area after 60-ML deposition. Features marked by arrows in (c) changed over a 2-min period.

Mg for the same region taken ~2 min apart. Changes were evident within the upper right area but the rest of the surface remained unchanged. Similar changes are evident in Figs. 4(c) and 4(d) for an $860 \times 860$ Å$^2$ area for a 60-ML Mg film. For images taken ~2 min apart, the screw dislocation marked by an arrow in Fig. 4(c) has been annihilated and steps developed in its place. These changes were probably not induced by the tip because only specific features changed and the resolution of the tip remained the same during scanning. Instead, we associated them with dislocation movement within the Mg film. The as-grown Mg films probably have nonequilibrium structures that are kinetically limited. Dislocation movement makes it possible to release internal strain. Such dislocation movement has been observed on a GaAs(110) surface using STM.[22] During these processes, atoms may leave or join a changing structure, causing growth or dissolution of 2D island structures, as observed.

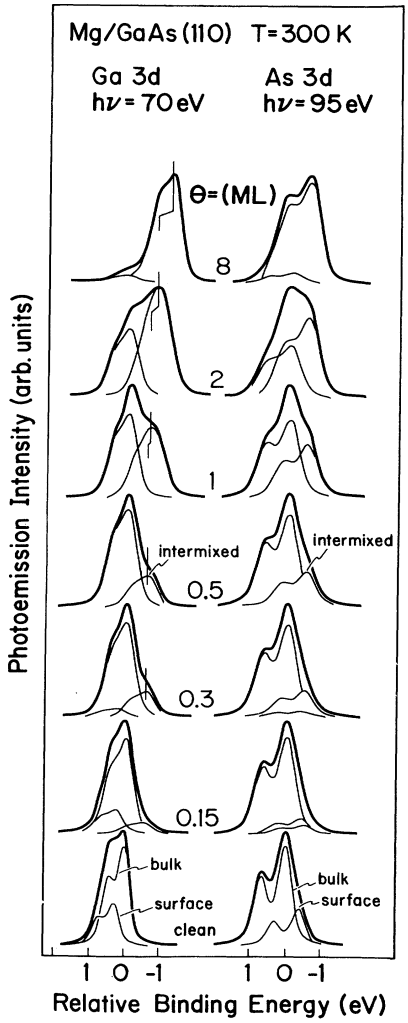


FIG. 5. Ga 3*d* and As 3*d* core-level EDC's for GaAs(110) with increasing Mg depositions at 300 K. The spectra are referenced in energy to the bulk component to emphasize the relative binding energy shifts of the reacted components. The intensity of each spectrum is background subtracted and normalized to the highest feature.

## INTERFACE CHEMISTRY

To understand the atomic bonding configurations associated with the growth structures discussed above, we must rely upon photoemission. Figure 5 shows Ga 3*d* and As 3*d* core-level EDC's for the clean surface where the familiar surface-shifted components appear at $-0.39$ eV for As and 0.28 eV for Ga. (The photon energies were chosen to give approximately the same inelastic scattering lengths.) With Mg deposition, new components appeared at lower binding energy for As and Ga, consistent with transfer of electron density from Mg to substrate atoms, in agreement with the STM results discussed above. As the Mg coverage increased, these components grew at the expense of the surface component. This is evident from the inset of Fig. 6 where the intensity of the Ga 3*d* surface component (normalized to that of the clean surface) is plotted as a function of Mg deposition. As shown, the surface component diminished steadily and was no longer distinguishable by ~0.5-ML deposition. This correlates well with the growth of the $2 \times 1$ struc-

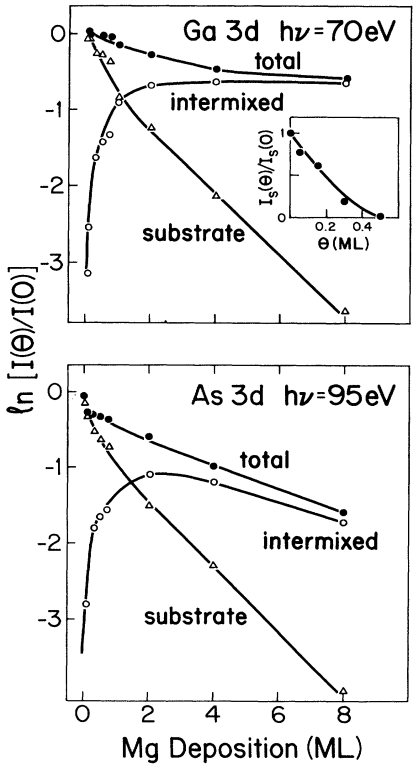


FIG. 6. Attenuation curves showing the intensity variations for the various Ga 3*d* (upper panel) and As 3*d* (bottom panel) core-level features as a function of Mg deposition. The inset shows the intensity of the Ga 3*d* surface-shifted component normalized to the intensity of the clean surface as a function of Mg coverage at low coverage as the Mg $2 \times 1$ structure grew. The persistence of As and, especially, Ga emission to high coverage demonstrates segregation to the surface region.

ture. The disappearance of the surface component by ~0.5 ML for Mg deposition stands in contrast to results for 2D overlayers such as Bi/GaAs(110) and Sb/GaAs(110).[23–25] In those cases, the surface structure was 1×1 and the surface component vanished with the completion of the first monolayer. This implies that the loosely packed 2×1 Mg structures change the electronic environment of all surface Ga and As atoms through bonding.

The markedly different rates of attenuation for the substrate and Mg-induced components after ~0.5 ML indicates that intermixing of Ga, As, and Mg atoms had been initiated. Figure 6 shows logarithmic plots of the intensities of the various components of Fig. 5 as a function of Mg deposition. The attenuation of substrate peak intensity, taken to be the sum of bulk and surface components, deviates from a straight line because of the conversion of the surface component into a chemisorbed component at low coverage and intermixing and cluster formation thereafter. The component associated with the intermixed species attenuates faster for As than for Ga because of differences in chemical trapping and solubilities.[26]

Intermixing is also evident from the EDC's of Fig. 5 where the intensity of the intermixed component grew relative to the substrate component, dominating by 1–2 ML and being the sole component evident by ~8 ML. The Ga line shape showed a sharpening with Mg deposition, and emission from Ga could be detected after 150-ML deposition. Such Ga behavior has been observed repeatedly for metal overlayer growth on GaAs(110),[26] and it is associated with the release of cations into the overlayer due to preferential reaction with the anion and subsequent cation surface segregation.

The Mg 2*p* core-level EDC's summarized in Fig. 7 for low coverage represent the chemisorbed atoms identified in the structures of Fig. 1. Although little change was observed between 0.05 and 0.5 ML, the line shape broadened and the peak shifted to higher kinetic energy (lower binding energy) by 2-ML deposition. The line shape representative of metallic Mg was then evident by ~8 ML. We note that a Fermi level cutoff was first detected at ~2 ML, indicating that the mixture of Mg, Ga, and As was metallic. After 30-ML deposition, the probe region was essentially pure Mg with some residual segregated Ga, and the Mg 2*p* EDC showed the asymmetry typical of a metal. At this point, As has been buried at the extended interface because no As 3*d* signal can be detected.

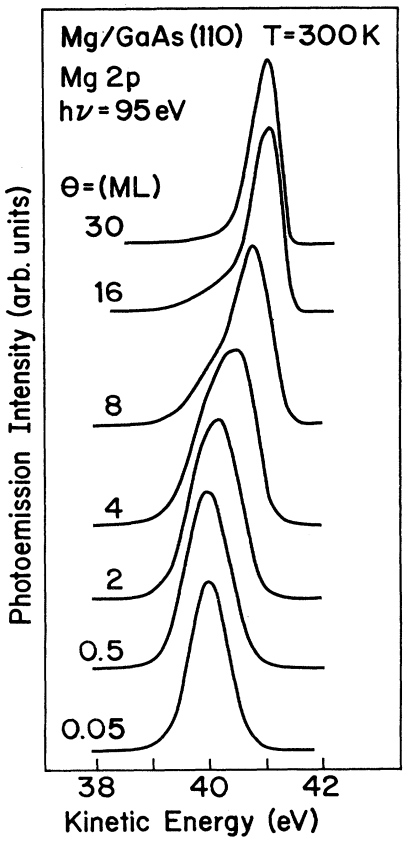


FIG. 7. Mg 2*p* core-level EDC's for representative Mg coverages. The spectra are plotted with kinetic energy as the horizontal scale. The clear change in line shape and shift with increased deposition shows the nucleation and growth of Mg in the intermixed layer. The results for 0.05-ML deposition reflect Mg bonds primarily in 2×1 structures depicted in Fig. 1.

## SUMMARY OF OVERLAYER GROWTH

A picture of the evolution of the Mg/GaAs(110) interface can be obtained by combining the results from STM and photoemission. At low coverage, a 2×1 structure forms, as shown in Fig. 1, and this structure induces surface changes so that atoms of the (110) responsible for the surface-shifted photoemission component adopt new bonding configurations. For this stable 2×1 structure, there is considerable charge transfer from Mg adatoms to the GaAs substrate but there is no apparent disruption of the substrate. For the GaAs(110) surface, individual Mg atoms are mobile but are trapped in 2D arrays by cooperative bonding to the surface. Additional Mg atoms deposited on the surface occupy sites within the loosely packed 2×1 structure. The resulting structure leads to an instability and Mg-Ga-As intermixing is initiated. This interface instability reflects the local number density of Mg atoms. The onset of reaction is similar to the cluster-induced reaction proposed by Zunger[27] and observed experimentally for Ce/Si(111) (Ref. 28) and Sm/GaAs(110).[8,20,29] Intermixing of Mg, Ga, and As yields reacted clusters and this reaction spreads across the surface. Once formed, the layer acts to kinetically impede continued reaction. Continued deposition facilitates crystalline formation on the interfacial layer, despite the presence of Ga atoms. The Mg film produced in this fashion is polycrystalline because of the randomness associated with cluster formation and coalescence. Dislocations within the film probably reflect disorder of the buried interface and strain associated with Mg film growth.

## ACKNOWLEDGMENTS

This work was supported by the National Science Foundation. The authors thank M. Chander for his assistance in the LEED experiments and T. R. Ohno for helpful discussions. The synchrotron-radiation studies were done at Aladdin, a user facility supported by the National Science Foundation and operated by the University of Wisconsin.

[1]R. J. Wilson and S. Chiang, Phys. Rev. Lett. **58**, 369 (1987); E. J. van Loenen, J. E. Demuth, R. M. Tromp, and R. J. Hamers, *ibid.* **58**, 373 (1987); R. J. Wilson and S. Chiang, *ibid.* **59**, 2329 (1987); St. Tosch and H. Neddermeyer, *ibid.* **61**, 349 (1988); A. Samsavar, E. S. Hirschorn, F. M. Leibsle, and T.-C. Chiang, *ibid.* **63**, 2830 (1989).

[2]U. K. Köhler, J. E. Demuth, and R. J. Hamers, Phys. Rev. Lett. **60**, 2499 (1988).

[3]J. Nogami, A. A. Baski, and C. F. Quate, J. Vac. Sci. Technol. A **8**, 3520 (1990); Appl. Phys. Lett. **58**, 475 (1991).

[4]R. M. Feenstra, Phys. Rev. Lett. **63**, 1412 (1989); J. Vac. Sci. Technol. B **7**, 925 (1989).

[5]C. K. Shih, Efthimios Kaxiras, R. M. Feenstra, and K. C. Pandey, Phys. Rev. B **40**, 10 044 (1989); C. K. Shih, R. M. Feenstra, and P. Mårtensson, J. Vac. Sci. Technol. A **8**, 3379 (1990).

[6]P. N. First, R. A. Dragoset, J. A. Stroscio, R. J. Celotta, and R. M. Feenstra, J. Vac. Sci. Technol. A **7**, 2868 (1989).

[7]P. N. First, J. A. Stroscio, R. A. Dragoset, D. T. Pierce, and R. J. Celotta, Phys. Rev. Lett. **63**, 1416 (1989); J. A. Stroscio, P. N. First, R. A. Dragoset, L. T. Whitman, D. T. Pierce, and R. J. Celotta, J. Vac. Sci. Technol. A **8**, 284 (1990); R. A. Dragoset, P. N. First, J. A. Stroscio, D. T. Pierce, and R. J. Celotta, in *Growth, Characterization, and Properties of Ultrathin Magnetic Films and Multilayers,* edited by Berend T. Jonker, Joseph P. Heremans, and Ernesto E. Marinero, MRS Symposia Proceedings No. 151 (Materials Research Society, Pittsburgh, 1989), p. 193.

[8]B. M. Trafas, D. M. Hill, R. L. Siefert, and J. H. Weaver, Phys. Rev. B **42**, 3231 (1990).

[9]B. M. Trafas, Y.-N. Yang, R. L. Siefert, and J. H. Weaver, Phys. Rev. B **43**, 14 107 (1991); J. H. Weaver and G. D. Waddill, Science **251**, 1444 (1991).

[10]J. C. Patrin, Y. Z. Li, and J. H. Weaver, unpublished STM results for Al growth on stepped and unstepped GaAs(110).

[11]D. Mao, K. Young, K. Stiles, and A. Kahn, J. Vac. Sci. Technol. A **7**, 744 (1989).

[12]Park Scientific Instruments, Mountian View, CA 94043.

[13]R. M. Feenstra, J. A. Stroscio, J. Tersoff, and A. P. Fein, Phys. Rev. Lett. **58**, 1192 (1987).

[14]C. M. Aldao, J. M. Vitomirov, F. Xu, and J. H. Weaver, Phys. Rev. B **37**, 6019 (1988); F. Xu, C. M. Aldao, I. M. Vitomirov, Z. Lin, and J. H. Weaver, *ibid.* **36**, 3495 (1987).

[15]G. K. Wertheim and S. B. Dicenzo, J. Electron Spectrosc. Relat. Phenom. **37**, 57 (1985); J. J. Joyce, M. del Giudice, and J. H. Weaver, *ibid.* **49**, 31 (1989).

[16]N. D. Lang, Phys. Rev. Lett. **58**, 45 (1987).

[17]R. J. Hamers, Annu. Rev. Chem. **40**, 531 (1989).

[18]J. Tersoff and D. R. Hamann, Phys. Rev. Lett. **50**, 1998 (1983); Phys. Rev. B **31**, 805 (1985).

[19]J. Ihm and J. D. Joannopoulos, Phys. Rev. B **26**, 4429 (1982).

[20]Y. Z. Li, J. C. Patrin, M. Chander, and J. H. Weaver, Phys. Rev. B (to be published), results for rare earth overlayers on GaAs(110).

[21]L. J. Whitman, J. A. Stroscio, R. A. Dragoset, and R. J. Celotta, Phys. Rev. Lett. **66**, 1338 (1991); Science **251**, 1206 (1991).

[22]G. Cox, D. Szynka, U. Poppe, K. H. Graf, K. Urban, C. Kisielowski-Kemmerich, J. Krüger, and H. Alexander, Phys. Rev. Lett. **64**, 2402 (1990).

[23]G. D. Waddill, C. M. Aldao, C. Capasso, P. J. Benning, Yongjun Hu, T. J. Wagener, M. B. Jost, and J. H. Weaver, Phys. Rev. B **41**, 5960 (1990).

[24]J. J. Joyce, J. R. Anderson, M. M. Nelson, C. Yu, and G. J. Lapeyre, J. Vac. Sci. Technol. A **7**, 850 (1989).

[25]F. Schäffler, R. Ludeke, A. Taleb-Ibrahimi, G. Hughes, and D. Rieger, J. Vac. Sci. Technol. B **5**, 1048 (1987).

[26]J. H. Weaver, in *Electronic Materials: A New Era of Materials Science,* edited by J. R. Chelikowsky and A. Franciosi (Springer-Verlag, Berlin, 1991), Chap. 8; J. H. Weaver, Z. Lin, and F. Xu, in *Surface Segregation Phenomena,* edited by P. A. Dowben and A. Miller (CRC, Boca Raton, FL, 1990), Chap. 10.

[27]A. Zunger, Phys. Rev. B **24**, 4372 (1981).

[28]M. Grioni, J. J. Joyce, S. A. Chambers, D. G. O'Neill, M. del Giudice, and J. H. Weaver, Phys. Rev. Lett. **53**, 2331 (1984).

[29]T. Komeda, S. G. Anderson, J. M. Seo, M. Schabel, and J. H. Weaver, J. Vac. Sci. Technol. A **9**, 1964 (1991).

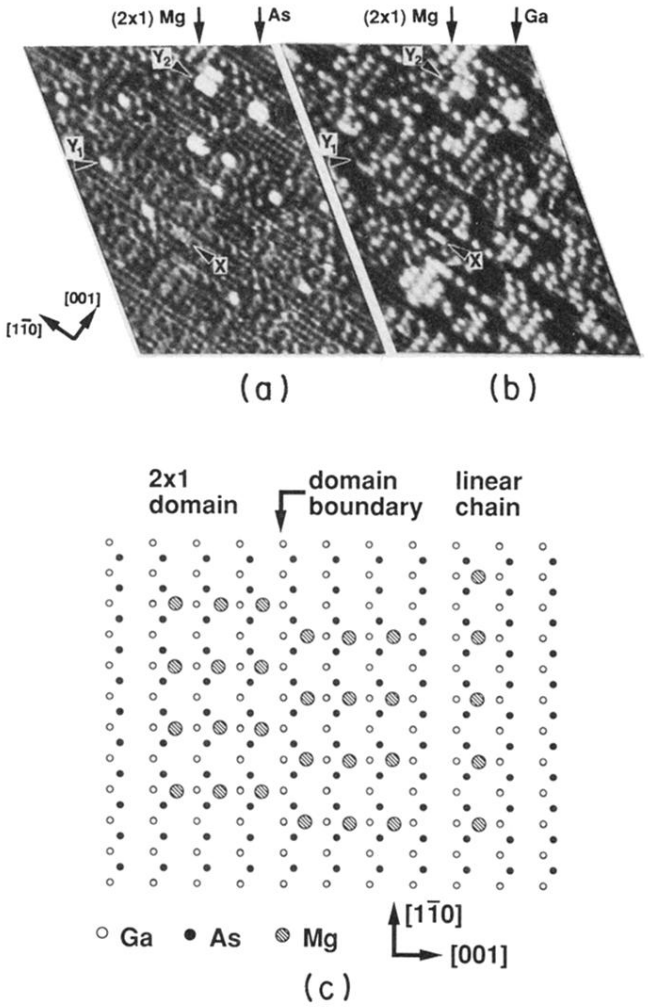


FIG. 1. STM images probing (a) occupied states and (b) unoccupied states of the same $140 \times 140$ Å$^2$ for 0.12-ML deposition of Mg on GaAs(110). The images were acquired with the tip biased by $\pm 2.4$ V and a constant tunneling current at 0.7 nA. Most Mg adatoms appear as individual bright features occupying the surface sites indicated in the schematic model of (c). The nearest-neighbor distances between Mg atoms are 8 and 5.65 Å along [1$\bar{1}$0] and [001] directions, respectively. The dominant structures reflect a local $2 \times 1$ array but linear chains along the substrate [1$\bar{1}$0] direction are also evident. The different brightnesses for Mg atoms in (a) and (b) reflect a higher density for unoccupied states than occupied states. Features marked *X* signal closer packing of Mg atoms in the [1$\bar{1}$0] direction while those marked *Y* signal nucleation of clusters.

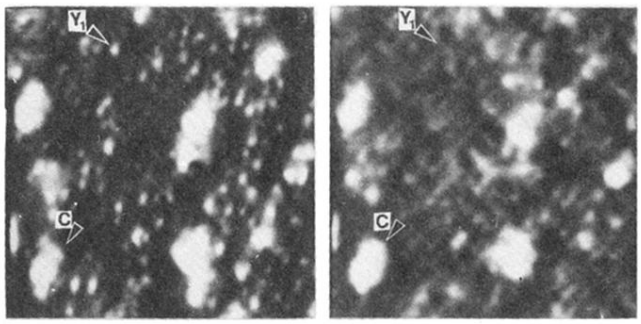


FIG. 2. STM images showing cluster formation after the deposition of the equivalent of 0.25 ML of Mg. The same $170\times170$ Å$^2$ was scanned with the tip bias of $\pm2.88$ V for (a) and (b), respectively, and a tunneling current of 0.15 nA. Clusters measuring $\sim20$ Å in diameter and 2–4 Å in height with no apparent internal structure (marked *C*) can be seen along with unperturbed $2\times1$ areas and *Y* features as in Fig. 1 (e.g., $Y_1$ marked). The photoemission results indicate that the clusters reflect intermixed regions containing Mg, Ga, and As.

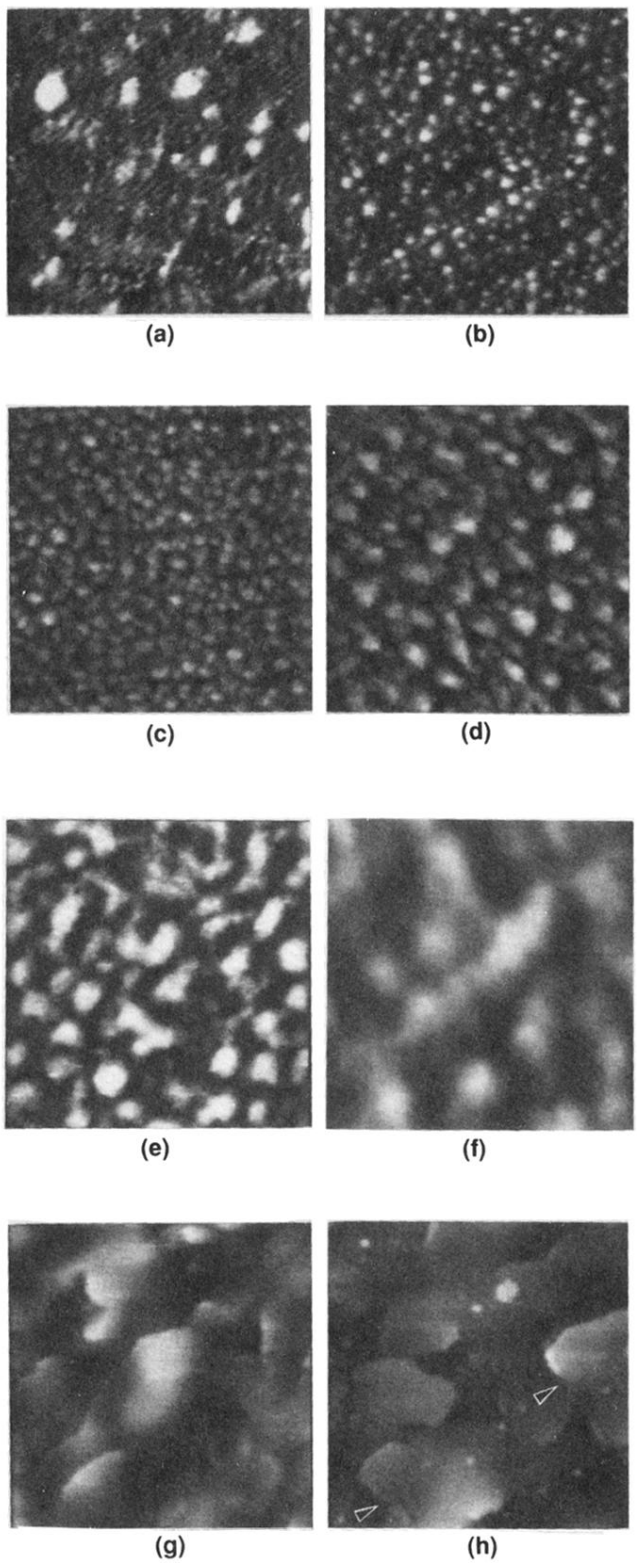


FIG. 3. STM images showing the evolution of the Mg/GaAs interface for deposition of 0.25, 0.38, 1.0, 3.0, 5.0, 7.5, 9, and 30 ML for images (a)–(h). The imaged region measured $290\times290$ Å$^2$ for (a) and $700\times700$ Å$^2$ for (b)–(h). Image (a) was acquired with a negative tip bias, but the others were taken with a positive tip bias. $2\times1$ structures observed at low coverages yielded to reacted clusters that grew laterally and eventually sealed the surface so that polycrystalline Mg film growth could occur. Arrows (h) indicate screw dislocations in the Mg film.

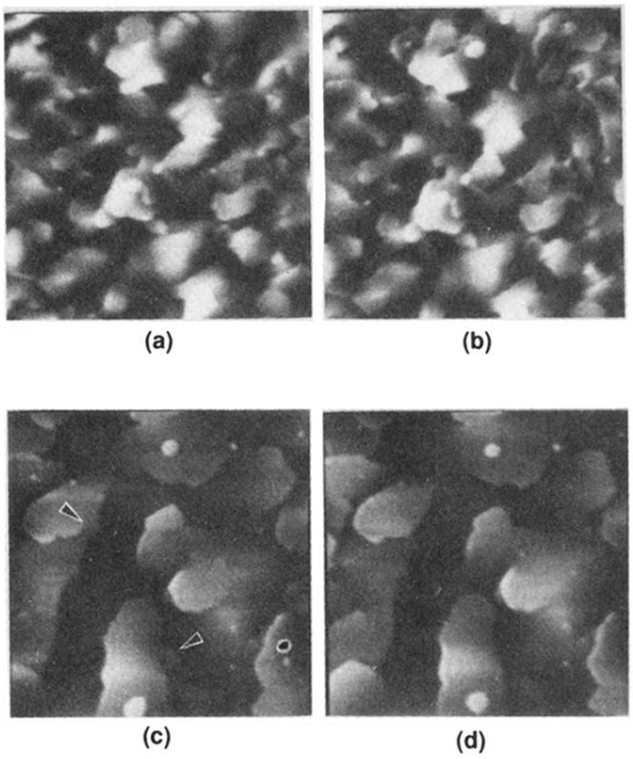


FIG. 4. These images highlight areas of structural instability and dislocation movement in the Mg thin films. Images (a) and (b) were taken ~2 min apart for the same 1400×1400 Å$^2$ area after 15-ML Mg deposition. Apparent structural changes occurred in the upper right portion. Images (c) and (d) were acquired from an 860×860 Å$^2$ area after 60-ML deposition. Features marked by arrows in (c) changed over a 2-min period.